Vesicular aggregation and morphologic evolvement of a flexible-rigid block hydrogen-bonding complex

Qingtao Liu, Yinglin Wang, Wen Li, Lixin Wu*

State Key Laboratory of Supramolecular Structure and Materials, College of Chemistry, Jilin University, Qianjin Street 2699, Changchun 130012, PR China

ARTICLE INFO

ABSTRACT

In this paper, we selected a flexible poly(ethylene oxide) (PEO) connected to a stilbazole head group and a semi-rigid dendron of gallic acid with three alkyl chains to prepare an amphiphilic complex through hydrogen bonding. The structure of flexible-rigid complex has been characterized by ^{1}H NMR, IR and DLS. From the calculation of the binding interaction, the bonded complex occupies ca. 59.5% of total amount of molecules at the molar ratio of 1:1 of its two components, accompanied by the stability constant K_{sc} about 369 L/mol. The complex displays vesicular aggregation in toluene mixed with a certain amount of DMSO and the structural characterization indicates a symmetrical bilayer with PEO component locating outside towards the solution based on the analysis of contact angle. More interesting, tubular architecture of the complex is observed and found with the similar bilayer structure as that of the vesicular aggregation. The tubules are confirmed to derive from the vesicular aggregation through aging the vesicular structure. It is believed that the present investigation is helpful for the understanding of the dynamics of the vesicle evolvement based on the flexible-rigid complex.

© 2008 Elsevier Ltd. All rights reserved.

1. Introduction

Supramolecular self-assembling has attracted considerable attention over recent years because it provides an effective method for the spontaneous generation of well-defined architectures through non-covalent interaction such as electrostatic, hydrogen bonding, π–π, hydrophobic and van der Waals interactions [1–3]. Various precisely designed building blocks such as low-weight molecules, macromolecules and molecular complexes have been applied for the purposes of nanostructure construction [4], biological function mimic [5], selective catalysis, drug delivery [6] and electronic device [7] etc. And many interesting self-assembled structures such as micelles, vesicles, fibrils and tubular aggregations have been created by using these building blocks [8–13]. Especially, the structural and morphological transitions between different organized assemblies are of great importance in both fundamental research and practical applications. A lot of recent results have been reported concerning the transformations between vesicle and micelle, nanotube and vesicle by employing amphiphilic peptides [14–16], biomolecules [17,18], diblock molecules [19,20], surfactants [21], as well as the change of near spheroidal hexameric nanocapsule based on pyrogallol[4]arenas [22]. Possible mechanisms are proposed to understand the transformations among those aggregations in aqueous and organic solutions [23]. However, most of the researches are concentrated on the micelle to vesicle or tube to vesicle transformation, and the research on the transition from vesicles to tube-like structures was still rarely reported. Most recently, the amphiphilic molecular complexes composed of flexible and rigid components attracted considerable attention because in the mean time providing a convenient preparation and diverse combination, as a building block, it is also favorable for the diversiform self-assemblies. Therefore, it is of interest to study the morphologic transition of organized assemblies formed with such kind of supramolecular complexes. Among those driving forces, hydrogen bonding hold a prominent position because of their directionality and versatility [24–27]. Especially, it plays a crucial role in biological systems such as RNA and DNA. The supramolecuar assemblies based on nucleolipids modified molecules represent elegant examples of hydrogen-bonding interactions in governing structure and even function. These assemblies are of fundamental interest, as well as clinical importance, since some of these assemblies are used for the in vitro and in vivo delivery of DNA [27b]. In most cases, multiple hydrogen-bonds are normally required to strengthen the connection between different components [28,29]. However, self-assembling structures constructed through single hydrogen-bond in solution [30,31], liquid crystal [25] and sol–gel system [32] have also been reported.

Considering the environment sensitivity of component structure, we tried to combine the components with large diversity in

* Corresponding author. Tel.: +86 431 85168499; fax: +86 431 85193421.
E-mail address: wulx@jlu.edu.cn (L. Wu).

molecular length, volume ratio, rigidity and flexibility as well as hydrophobic and hydrophilic properties together to build a complex through single hydrogen bonding. By selecting suitable hydrogen-bond donor–acceptor pair, we prepared a complex with a rigid two generation dendritic block and a flexible poly(ethylene oxide) with stilbazole head group and realized the morphologic control of its aggregates in solution through carefully tuning solvent polarity and concentration in the previous research [33]. To be a successive work, in this paper, by changing the dendritic component to one generation, we found that its hydrogen-bonding complex with the same flexible component formed vesicles and tubules, which are similar with other single component building blocks. We herein report the preparation of the components and the complex, as shown in Scheme 1; the vesicular and nanosized tubular aggregations and the transformation between them. We believe that the present investigation is benefit for the further understanding of the growth of nano-tubules from their mother vesicles.

2. Experimental section

2.1. Materials preparation

The two components applied to prepare the complex, trans-4-{2-[4-olig(oxyethylene)oxyphenyl]vinyl}pyridine (Py-EO$_{12}$) and 3,4,5-triscetyloxybenzoic acid (TCB-COOH), were synthesized as previously described [33]. The detailed procedure for the preparation of TCB-COOH and the analogue of the hydrogen-bonding complex, 4[4′-olig(oxyethylene)biphenylyloxy]-3,4,5-triscetyloxybenzal ether (PEO–Bph–TCB), is described in Supporting information. All solvents were purified and dried before use.

2.2. Sample preparation

Py-EO$_{12}$ and TCB-COOH with equivalent molar ratio, dissolved in chloroform, respectively, were mixed together, and the solvent was removed under reduced pressure after 10 min of sonication at room temperature. The residue was then redissolved in benzene and the tiny water contained in the residue was then removed by its azeotropy with benzene. Following this, the dried residue was dissolved in a certain volume of toluene, giving a sample solution of
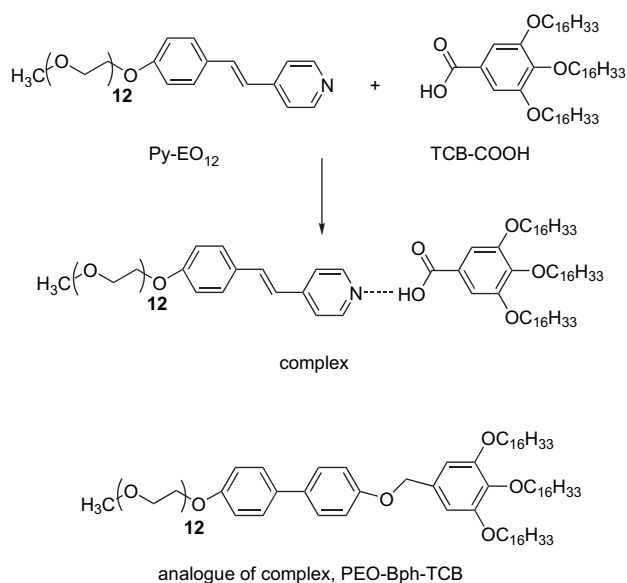
the complex with a transitory sonication. The aggregations in the mixed solution were prepared by the addition of other solvent such as dimethyl sulfoxide (DMSO) or acetone through encountering a short-time sonication. The species for transmission electron microscopy (TEM) were prepared by dropping the sample solution onto a carbon-coated copper grid, and the excess solvent was removed by suction with a piece of filter paper. Samples for scanning electron microscopy (SEM) were prepared by depositing a layer of gold on the very thin sample films. The species for atomic force microscopy (AFM) were obtained by casting the sample solution on a silicon wafer and quickly removing the excess solvent with filter paper. The samples for FT-IR were prepared by casting the concentrated sample solution onto a KBr pellet.

2.3. Measurements

FT-IR spectra were collected on a Bruker IFS66 V FT-IR spectrometer equipped with a DGTS detector (256 scans) with a resolution of 4 cm^{-1}. SEM measurement was carried out on a JEOL FESEM 6700F electron microscope operated at an accelerating voltage of 25 kV. AFM measurement was carried out on commercial instruments Nanoscope III and Dimension 3000™ from Digital Instrument Co., operating in tapping mode at room temperature in air. TEM images were obtained on a HITACHI H 8100 TEM instrument with the accelerating voltage of 200 kV. The giant vesicles were observed using a fluorescent microscope (Leica DMLP, Germany) with the ultraviolet radiation as an exciting source. Contact angle analysis was performed on a DSA 10 MK2 (droplet of 1 μL). The dynamic light scattering (DLS) was carried out on a Wyatt DAWN EOS Enhanced Optical System at 20 °C. UV–vis spectra were collected on a Shimadzu UV3100PC spectrometer.

3. Results and discussion

3.1. Structure characterization of hydrogen-bonding complex

As we employ the complex as the building block to fabricate organized aggregations, it is necessary to evaluate the binding between the two components in the complex. Here, the component TCB-COOH bearing a carboxyl terminal can serve as the proton donor, and the component Py-EO$_{12}$ containing a stilbazole group can be the proton accepter. Thus, TCB-COOH and Py-EO$_{12}$ could bind together through hydrogen bonding. The interaction can be effectively detected by ^{1}H NMR as the chemical shifts of the protons in stilbazole are sensitive to the bindings of proton and metal ions to pyridyl N atom [34]. As shown in Fig. 1, all protons in the two components appear in their definite chemical shifts. It should be noted that there is a very few stilbazole groups existing in *cis*-structure in the solution due to the exposure of the sample to the day light. Significantly, the chemical shifts of proton H-1 and H-2 in pyridyl group, and H-3 of vinyl group on the side close to the pyridyl move down field obviously with the addition of TCB-COOH. Besides the moving of chemical shift, the proton peaks become broader clearly as well. Other chemical shifts of protons in both of the components change very little due to little effect of the binding interaction to them. The formation of hydrogen bonded complex in the solutions can be further confirmed through the analysis of DLS measurement. When keeping the concentration of the mixture and each of two isolated components all at 2×10^{-4} M in toluene, we did not observe any definite aggregates for pure Py-EO$_{12}$. In contrast to this, pure TCB-COOH shows an aggregation with a hydrodynamic radius (R_h) of 320 nm, while obviously larger aggregation with R_h of 457 nm appears in the mixture (Fig. S1). Such a difference indicates that it is the cooperative interaction between Py-EO$_{12}$ and TCB-COOH resulting in the size increasing of the aggregates, which supports the presence of the complex that is
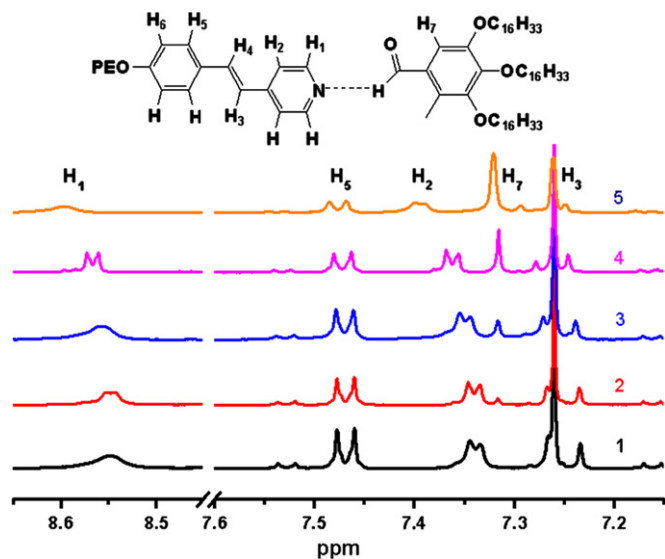

Scheme 1. Chemical structures of the complex and its relative components and structural analogue.

Fig. 1. ^1H NMR spectra of (1) pure Py-EO$_{12}$, and (2)–(5) the mixture with different molar ratios of TCB-COOH and Py-EO$_{12}$ at 1:8, 1:3, 1:1, and 3:1 in deuterated chloroform, respectively.

derived from hydrogen bonding in diluted solution [30,35,36]. In addition, by dropping the mixture solution onto the KBr pellet, the hydrogen bonding in the complex was also examined by IR spectra qualitatively. The shifting of C=O stretching vibration of TCB-COOH from 1681 cm^{-1} in its isolated state to 1701 cm^{-1} in the mixture and the disappearance of O–H stretching band at 3342 cm^{-1} provide clear evidences for the formation of hydrogen-bond between TCB-COOH and Py-EO$_{12}$ [37]. The IR data are listed in Supporting information.

As the chemical shifts of protons in Py-EO$_{12}$ are correlated to the concentration of TCB-COOH, we estimated the stoichiometry of the two components from the plot of frequency shifting versus the molar ratio of TCB-COOH to Py-EO$_{12}$ in the given region of the concentration, as shown in Fig. 2. From the turning point we know that the ideal molar ratio to make all Py-EO$_{12}$ hydrogen bonded is ca. 1.5 by elongating two linear increasing regions of the band shifting versus the molar ratio of the two components. At the molar ratio of 1:1, the bonded complex occupies ca. 59.5% of total amount of molecules, implying that the combination between the two components is dominant on comparison with other single
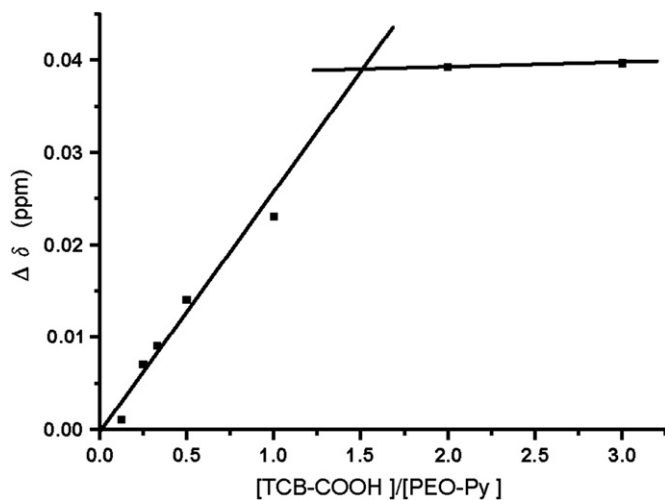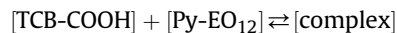

Fig. 2. Experimental plot of H$_2$ chemical shifts (corresponding to that of pure Py-EO$_{12}$) versus the mole ratio of TCB-COOH and Py-EO$_{12}$.

hydrogen-bonding complexes. In addition, we further calculated the stability constant of the complex based on the following reaction equation:

$$[TCB\text{-}COOH] + [Py\text{-}EO_{12}] \rightleftharpoons [complex]$$

$$
\begin{aligned}
K_{sc} &= \frac{[complex]}{[TCB\text{-}COOH][Py\text{-}EO_{12}]} \\
&= \frac{[complex]}{([TCB\text{-}COOH]_0 - [complex])([Py\text{-}EO_{12}]_0 - [complex])}
\end{aligned}
\tag{1}
$$

where [TCB-COOH], [Py-EO$_{12}$] and [complex] represent the concentration of TCB-COOH, Py-EO$_{12}$ and the complex at equilibrium state, respectively; [TCB-COOH]$_0$ and [Py-EO$_{12}$]$_0$ denote the starting (total) concentration of TCB-COOH and Py-EO$_{12}$ in the solution, respectively. To obtain the ratio of bonded amount to the total Py-EO$_{12}$, we defined

$$\theta = \frac{[Py\text{-}EO_{12}]}{[Py\text{-}EO_{12}]_0} \tag{2}$$

It can also be expressed as:

$$\theta = \left(\delta_{obs} - \delta_{Py\text{-}EO_{12}}/\delta_{complex} - \delta_{Py\text{-}EO_{12}}\right) = \left(\Delta\delta_{obs}/\Delta\delta_{complex}\right).$$

Here, δ_{obs} is the chemical shift of H$_2$ of Py-EO$_{12}$ in the mixture, $\delta_{Py\text{-}EO_{12}}$ is the chemical shift of H$_2$ of isolated Py-EO$_{12}$, and $\delta_{complex}$ is supposed to be the chemical shift of H$_2$ of Py-EO$_{12}$ that have completely recognized TCB-COOH, $\Delta\delta_{obs}$ denotes the difference of chemical shift of Py-EO$_{12}$ between the mixture and the isolated state, $\Delta\delta_{complex}$ is supposed to be the remains of chemical shift of all Py-EO$_{12}$ in bonded state after subtracting the value in isolated state. When applying M as the concentration ratio of TCB-COOH and Py-EO$_{12}$ in the solution, we can get

$$M = \frac{[TCB\text{-}COOH]_0}{[Py\text{-}EO_{12}]_0} \tag{3}$$

Combining Eqs. (1)–(3), we obtain

$$K_{sc} = \frac{\theta}{(M - \theta)(1 - \theta)[Py\text{-}EO_{12}]_0} \tag{4}$$

From the plot of Fig. 2, $\Delta\delta_{complex}$ is calculated to be ca. 0.0391 ppm. $\Delta\delta_{obs}$ is calculated to be ca. 0.0232 ppm, and thus θ is estimated to be ca. 0.595. Therefore, the stability constant K_{sc} is deduced to be about 369 L/mol, indicative of quite stable hydrogen bonding of the complex.

3.2. Vesicular aggregation

Because Py-EO$_{12}$ is a flexible block composed of hydrophilic EO chain binding to stilbazole head and TCB-COOH is a semi-rigid dendron composed of benzoic acid containing three hydrophobic alkyl chains, the complex of the two components exhibits integrated flexible-rigid and amphiphilic properties. Here, the difference of flexible and rigid properties can afford effective adjustment to the aggregation of the complex; the change of geometric shapes is favorable for diverse aggregation morphologies; the opposite dissolvability to the solvent provides additional driving force for the organization of the complex and the phase separation between the two components. In addition, the hydrogen bonding offers a sufficient freedom to the connection of the two parts in the complex. These features make the complex develop into interesting aggregations in solution. In pure toluene, the complex only forms slice-like aggregations with the water contact angle of 55° (Fig. S3). However,

giant globular aggregations are observed after the addition of a bit of polar solvent DMSO into the toluene solution, as shown in TEM image of Fig. 3a. The globular aggregation is obviously derived from the complex because it is completely different from each of two pure components alone under the same condition (Fig. S4). SEM data also illustrate that the pure Py-EO$_{12}$ is amorphous while pure TCB-COOH forms cylindrical fibres. The different aggregated morphologies between the complex and two isolated components confirm again the formation of hydrogen-bonding complex.

The globular aggregation could be further affirmed to possess a vesicular structure. As shown in Fig. 3b, the formed dent morphology appeared on SEM image due to the collapse of giant globular aggregates during the drying process, clearly indicates the hollow aggregated structure. To further prove the aggregation morphology, we added a fluorescent dye, 1×10^{-4} M of acridine orange, into the solution of complex. Giant green rings are observed remarkably from the fluorescent micrograph shown in Fig. 3c, illustrating that the dye molecules accumulate on the shell of the globular aggregation, which is in agreement with the hollow globular morphology observed in SEM image (for interpretation of the references to colour in text, the reader is referred to the web version of this article). The DLS measurement shows the size distribution of the globular aggregation with the diameter of ca.

1.9 μm in the mixed solution of 1×10^{-3} M (20/1 volume ratio of toluene to DMSO) (Fig. 3d), which is coincident to the TEM result under the same condition. As normally adopted in high resolution TEM measurement [38], from the amplified image (Fig. S5), we estimated that the vesicle possesses a layer thickness of ca. 11–14 nm, just approximately double the length of the ideal structure of the complex. The phospholipid and similar amphiphilic molecules are apt to self-assemble into vesicles with a symmetrical bilayer in selective solvent (but the bolaamphiphiles self-assemble into vesicles with a monolayer structure) [39]. Therefore, the wall of the self-assembled vesicular structure should have a symmetrical bilayer. However, the X-ray diffraction measurement shows no clear diffraction pattern, indicating a quite disordered layered structure in solid state probably. Furthermore, water contact angles were employed to identify the bilayer structure, and they are 136°, 29.3° and 37.1° for pure TCB-COOH, Py-EO$_{12}$ and the complex, respectively. As the contact angle of the complex is much smaller than that of pure TCB-COOH but much close to that of pure Py-EO$_{12}$, we believe that the hydrophilic EO block in the bilayer locates outside towards the solution. And thus, it is obvious that the addition of DMSO is crucial for the vesicular aggregation through enhancing the hydrophobic interaction between alkyl chains. The reason is that the increased polarity of the solvent is favorable for
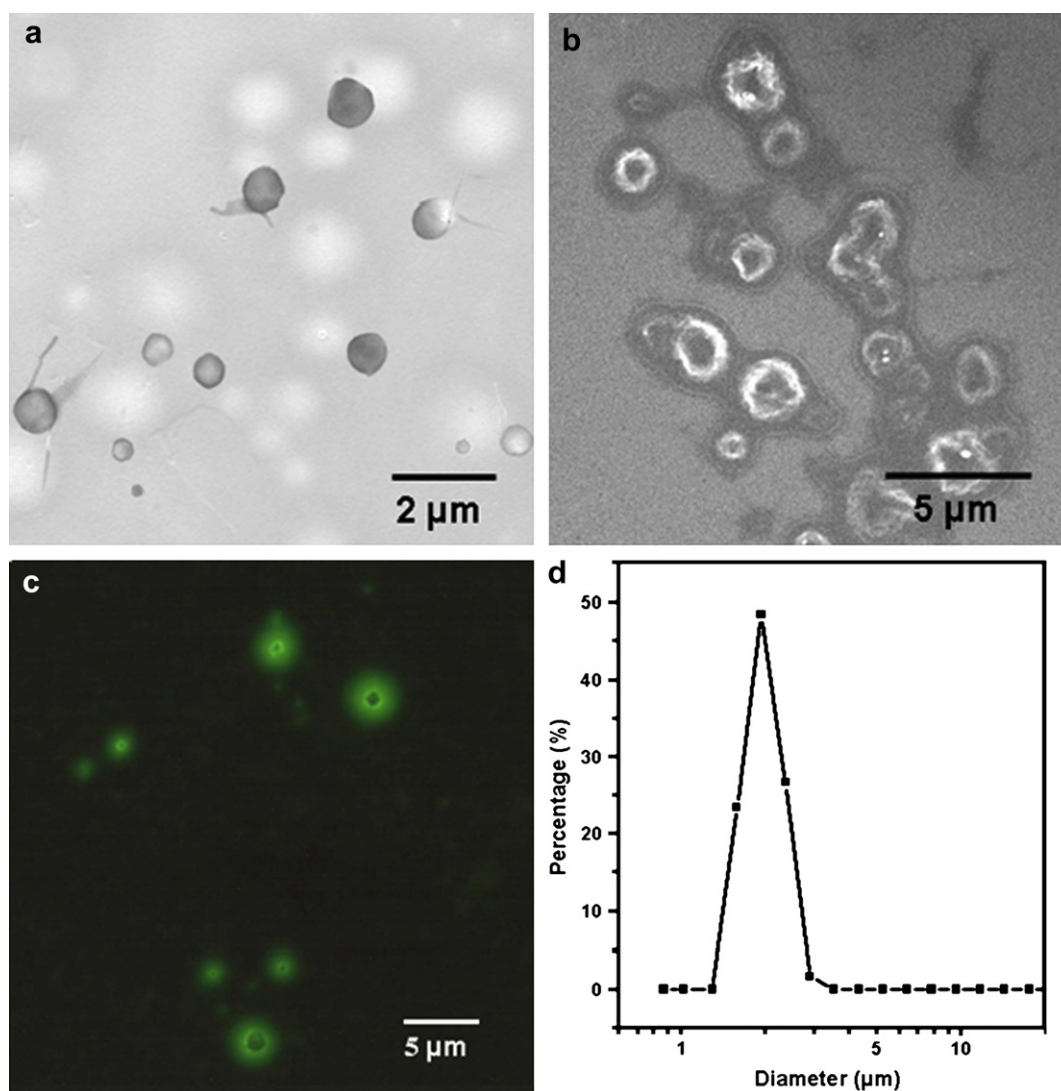
Fig. 3. Microscopic images and size distribution of the giant complex vesicles: (a) TEM and (b) SEM images of the casting film of the complex mixed solution; (c) fluorescent microscopic photograph of the casting film of the complex in the mixed solution with acridine orange dye; and (d) DLS graph of size distribution of the complex aggregation.
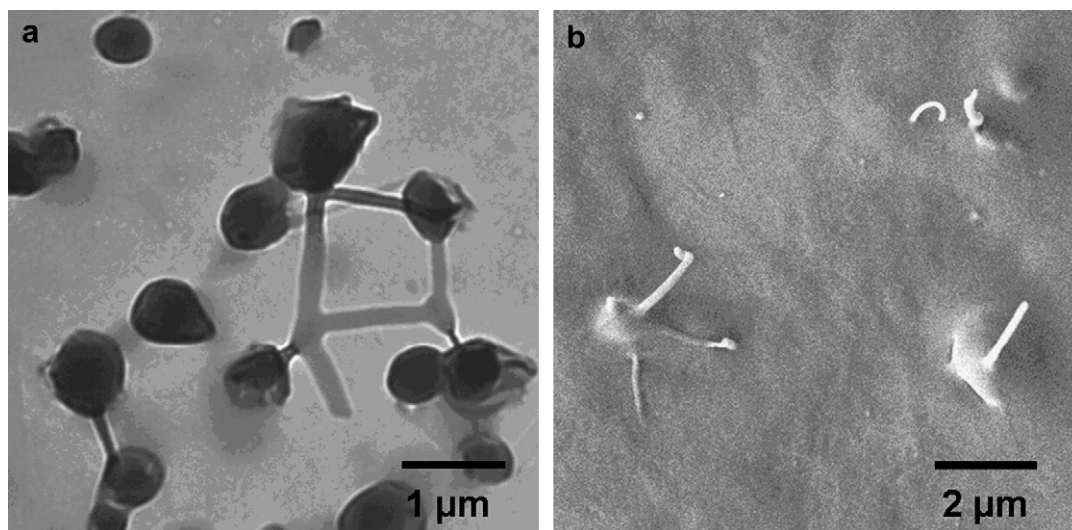
Fig. 4. (a) TEM and (b) SEM images of the wire-like aggregations of the hydrogen-bonding complex.
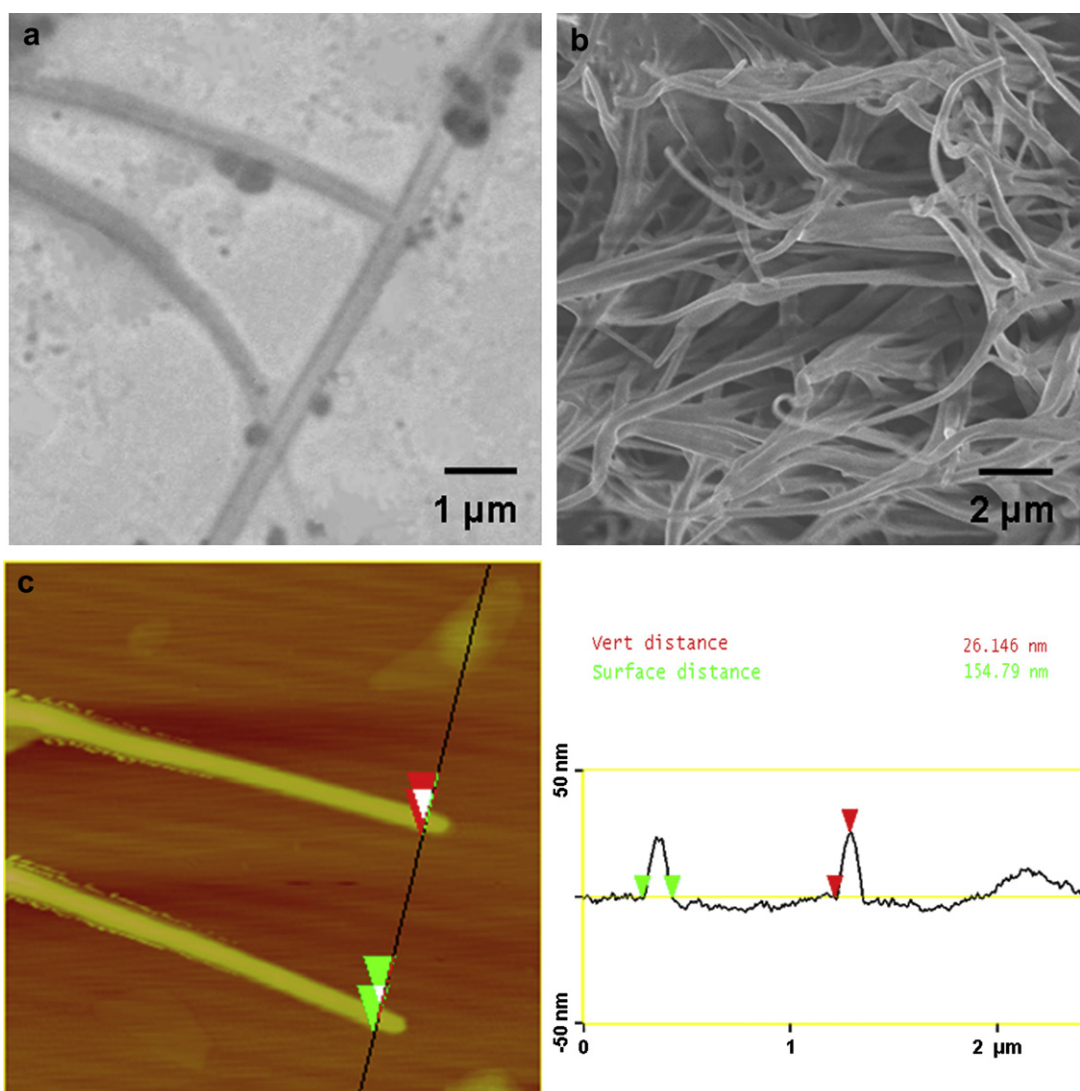

Fig. 5. (a) Amplified TEM image of the tubular aggregations; (b) SEM image of the tubular aggregations prepared by casting sample solution on the silica substrate and (c) AFM height image of selected tubular aggregations.
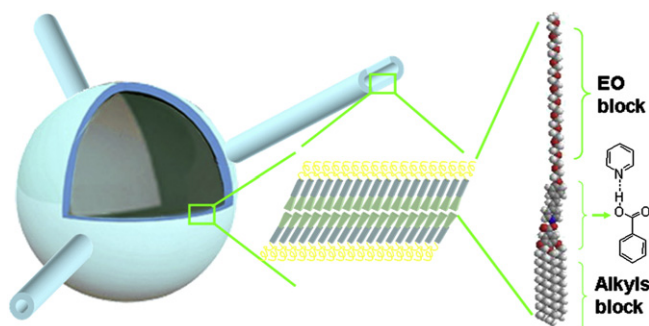
Fig. 6. Schematic structural model of the vesicular and tubular aggregations.

the proposed bilayer based on the fact that a little bit larger contact angle is favorable for the slice-like aggregation of the complex in pure toluene.

Generally, various self-assembled morphologies of amphiphilic molecules may be predicted theoretically. Israelachivili and coworkers proposed that the optimal surface area per polar head group depends on the packing parameter P, $P = v/(a_0 l_c)$, where v is the volume of the hydrophobic chain, a_0 is the surface area of polar head at the critical micellar concentration (cmc) and l_c denotes the molecular length. If $1/2 < P < 1$, bilayers with a spontaneous curvature (vesicles) are dominant; if $P = 1$, planar bilayers will be favored [8]. According to this prediction, regular tubular or vesicular structures may be constructed by accurately adjusting the configuration of hydrophilic and hydrophobic block of the complex. As the calculated volume ratio, $f_{(vol)}$ of the hydrophilic block in the complex is 0.56, the curved bilayer with the hydrophilic part packing towards outside should be the main existing state [40]. This estimation is in agreement with the regulation that the block possessing larger volume should locate at the outer part of the aggregation to satisfy the requirement by decreasing the surface of aggregation.

To demonstrate that the formation of vesicular aggregation is derived from the hydrogen-bonding complex rather than the isolated components or the mixture, we prepared a covalent bonded analogue of the complex, PEO-Bph-TCB, where the PEO and dendron blocks have the same chain length. Although the stilbazole was replaced by biphenyl group for avoiding the ionization of N atom, we believe that the analogue has a similar chemical structure geometrically and its aggregation feature should resemble that of the complex. PEO-Bph-TCB can also self-assemble into vesicular structure under the same condition (Fig. S6), and its water contact
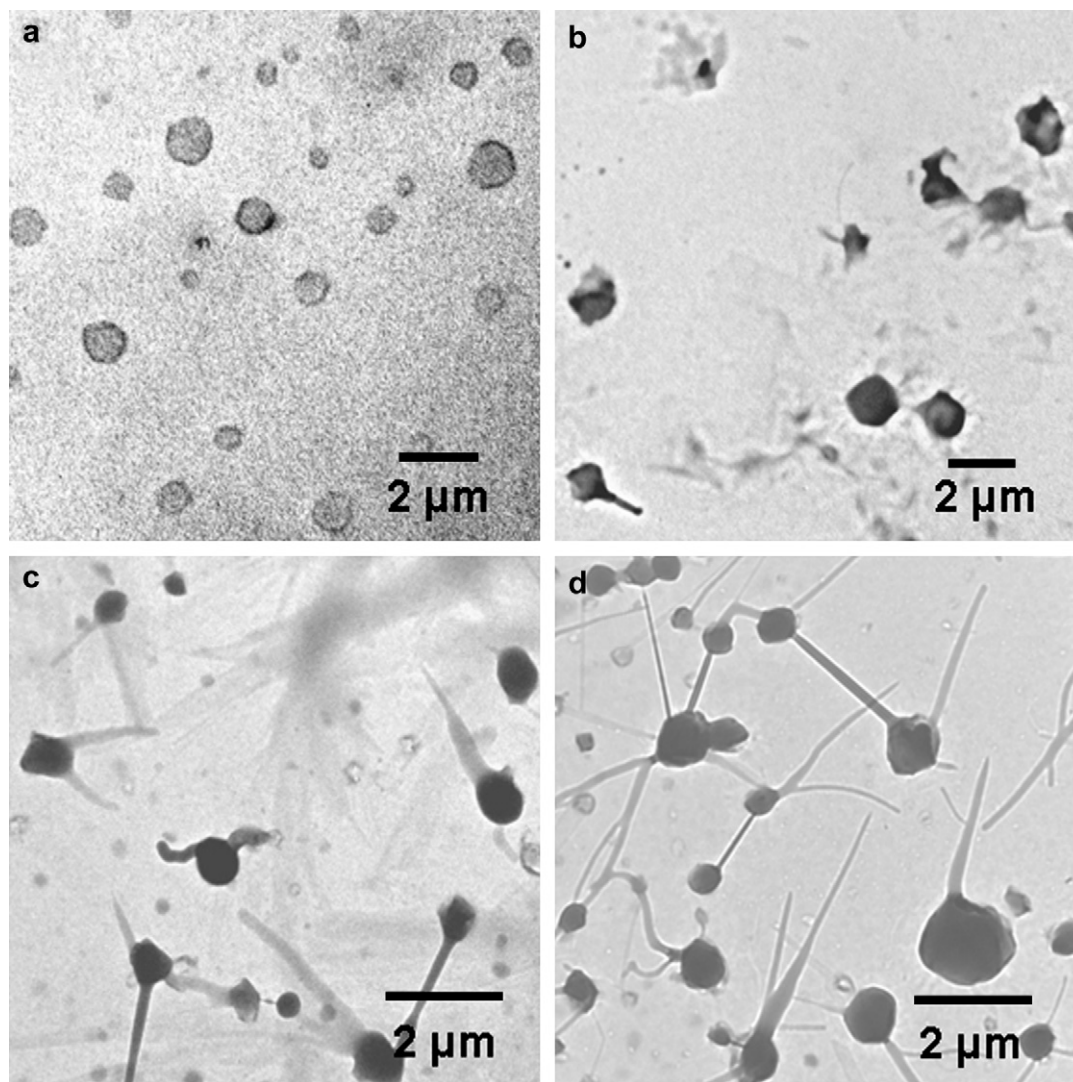

Fig. 7. TEM images of the growing process of nanotubes from the giant vesicle at −5 °C after (a) 1 day, (b) 2 days, (c) 3 days, and (d) 1 week standing, respectively.

angle is measured to be ca. 16.7°. This value is even lower than that of the complex, implying a hydrophilic surface of the vesicle. Based on these facts, we therefore believe that the aggregation in the case of two-component system is derived from the whole building block of the hydrogen-bonding complex because both the complex and the analogue form the vesicular structure with the EO block locating outside and the TCB block inside of the aggregation structure.

3.3. Tubular aggregation

Interestingly, besides the giant vesicular architecture, we also found wire-like structure attaching to the vesicular aggregation, as demonstrated by TEM, and SEM measurements shown in Fig. 4. Generally, comparing with the periphery, both the vesicles and tubular wires should display the nature of a higher transmission at the central part of the aggregation due to their hollow structures. From the further observation of TEM in Fig. 5a, the configuration of the dark edge for the wire-like structure with a size of 100–300 nm in width and up to a few micrometers in length suggests a tubular aggregation even though we failed to observe the lateral cavity. The wall thickness, ca. 11–14 nm estimated at the edge of the wire-like structure, is in consistent with the single molecular bilayer

estimated from the observed vesicles (see Supporting information). The SEM image of the complex prepared by casting the mixture solution, as shown in Fig. 5b, exhibits similar aggregation morphologies as those observed in TEM measurement. The height and diameter of tubular aggregates are found to be about 26 and 135 nm on average, respectively, from AFM result. The short height comparing with the long diameter implies a subsided structure and its value is just in accordance with double the layer thickness estimated from TEM, further supporting the dent tubular structure. Therefore, we suggest that both the tubules and the giant vesicles possess the same bilayer structure and the corresponding schematic drawing is presented in Fig. 6 [41].

The packing structure of stilbazole group in the aggregation of the complex was examined by UV–vis spectrum. Both the tubule–vesicle networks and complete vesicular aggregations show nearly identical absorption band at 319 nm, showing a small blue-shift in comparison with the band at 325 nm for free stilbazole group in chloroform. Such a shifting is definitely not resulting from the hydrogen bonding because in the same condition the spectra of pure Py-EO$_{12}$ with and without the addition of an acid (acetic acid is employed in the measurement) show the identical band position (Fig. S7). Therefore, the stilbazole group can be concluded in the H-aggregation state.
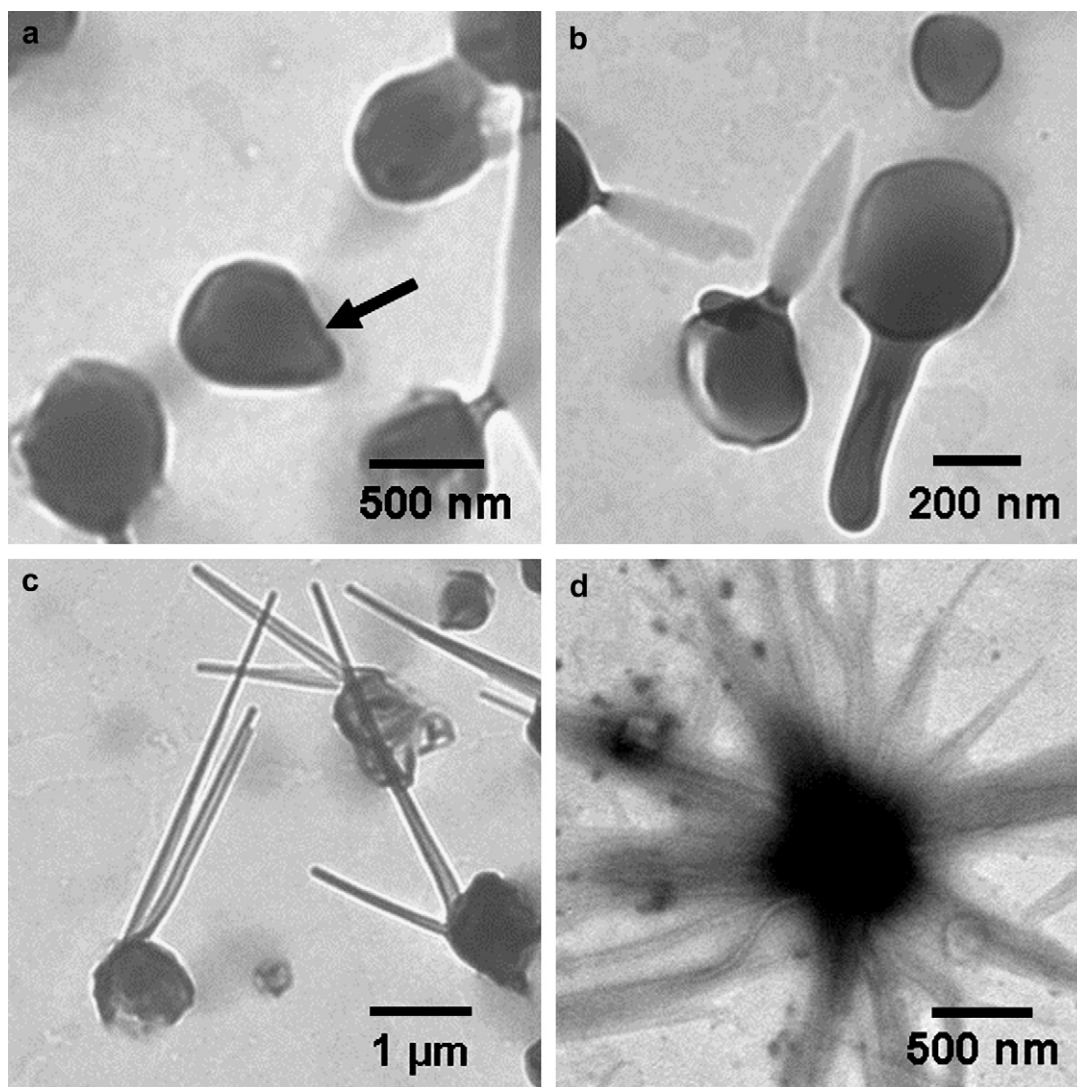
Fig. 8. Typical TEM images of nanotubes under various growing stages: (a) at the initial growing state, protruding from the wall of the giant vesicle to form a pear shape; (b) rudiments of the nanotubes just with inhomogeneous diameters; (c) grown long nanotubes with whole vesicles; and (d) pure nanotubes accompanied by the languishment of vesicles located at the center. These images are selected from those samples at the equilibrium state at room temperature.

3.4. Evolvement of vesicular to nanotubular aggregation

As the tubular aggregation is always found attached to the vesicles (Figs. 3 and 4), it is believed that there is a transformation process between the two aggregation morphologies. To identify that the growth of the tubular aggregation is sourced from vesicles, we examined the complex solution after having encountered 1, 2, 3 and 7 days of standing by TEM. To decelerate the transformation process of the aggregation, we prepared the fresh complex solution at −5 °C. The vesicular aggregation begins to appear after 1 day of standing, as observed in Fig. 7a. Meanwhile, the shape of vesicles starts to change and the short tubular aggregation is found growing from the vesicle after 2 days of standing for the sample, as shown in Fig. 7b. More tubules appear and grow much longer from the vesicles after 3 days standing, as illustrated in Fig. 7c and d. As for the sample after 1 week of standing, the growth of the tubules reaches their utmost and the length of the tubular aggregations increases up to micrometer scale. Thus, TEM observation versus the aging time clearly proves that the tubular aggregations are evolved from vesicular aggregation.

In addition, various intermediate states during the growth of tubules from vesicles are captured by TEM at room temperature, which is helpful for understanding the evolving process of the tubules. The protuberance was found to appear on vesicular aggregations in the beginning stage of the transformation, as shown in Fig. 8a. Such protuberance grows gradually into an extended structure (Fig. 8b), and in some cases the vesicles seem to leak and something flows out from the breach. Then a tubular aggregation forms through a shrinking of its size from the surface of the vesicle, implying that the tubules might be derived from the fission of the vesicle. When the grown tubules are few, the mother vesicles keep still in their whole state, as shown in Fig. 8c. But when the amount of grown nanotubules becomes more, the mother vesicles collapse and only non-structured aggregations are left at the original sites (Fig. 8d). In general, the mother vesicles generate protrusions which then separate from the main object, developing into two isolated vesicles [42] or fissuring to form a small daughter vesicle [43]. However, in the present case, the filial generation evolved from the vesicles becomes the nanosized tubules, rather than the normal daughter vesicles. Therefore, we suggest that the initial tubules may form from the growth of protrusion as a pearling phase from the wall of the vesicles, which is different from a simple cleavage such as a fission of daughter vesicles from the mother one or the fusion of the same vesicles into the tubules [19,20,44].

To the best of our knowledge, the evolvement of the nanosized tubules from vesicles and the tubule-crosslinked vesicle networks have been rarely reported [22,45]. In fact, we are still not sure of the definite mechanism and the initial driving force regarding the formation and evolvement of the tubular aggregations. We suggest that the hydrogen bonding should be responsible for the formation of tubules in the process of fission because we did not find any tubules grown from the aggregation of the analogue of the complex. It should be noted that the vesicle-nanotubes network is valuable to the field of biologic function mimic, such as the model research of nerve fibres [46]. The addition of other non-proton polar solvents, such as acetone or dimethyl formamide, into the toluene solution of the complex can also induce the formation of vesicles although we did not observe the growth of nanotubes from the vesicles. A possible explanation for the role of polar solvents to the formation of giant vesicles may be that the complex with similar volume of the two blocks tends to form lamellar bilayer structure. The insertion of polar solvent into EO block could increase the volume of the hydrophilic part and thus decrease the value of P, leading to the spontaneous bending of the bilayer structure and the formation of giant vesicles [47]. We believe that the higher flexibility of the complex than that of its analogue should be favorable for the fission of the vesicles and thus promoting the growth of the nanosized tubular aggregation.

4. Conclusion

By employing a flexible poly(ethylene oxide) connected to the stilbazole and a semi-rigid dendron with alkyl chains, we prepared an amphiphilic complex through hydrogen bonding. This complex exhibits self-organized property and forms vesicular aggregation in toluene solution containing a little amount of DMSO in contrast to undefined and fibrous aggregation of its two isolated components. It's believed that the structure of the vesicles consists of bilayer of the complex, where the flexible part is located outside towards the solvent and the rigid part is inside the aggregation. The interesting tubular aggregation of this hydrogen-bonding complex is found in the mean time and it is revealed to derive from the initial vesicles. The analysis to the structure suggests that the tubular aggregation possesses the similar stacking structure to that of vesicle of the complex. We think that the present investigation is helpful for the understanding of the dynamic process of the vesicle evolvement to the nanosized tubules.

Acknowledgement

Appendix. Supporting information

Supporting information associated with this article can be found in the online version, at doi:10.1016/j.polymer.2008.07.052.

References

[1] Lehn J-M. Supramolecular chemistry. New York: VCH Press; 1995.
[2] Service RF. Science 2005;309:95.
[3] Alper J. Science 2002;295:2396–7.
[4] Elemans JAA, Rowan AE, Nolte RJM. J Mater Chem 2003;13:2661–70.
[5] Keizer HM, Sijbesma RP. Chem Soc Rev 2005;34:226–34.
[6] Jang W-D, Nishiyama N, Zhang G-D, Harada A, Jiang D-L, Kawauchi S, et al. Angew Chem Int Ed 2005;44:419–23.
[7] Schenning APHJ, Meijer EW. Chem Commun 2005:3245–58.
[8] Shimizu T, Masuda M, Minamikawa H. Chem Rev 2005;105:1401–44.
[9] Uzun O, Sanyal A, Nakade H, Thibault RJ, Rotello VM. J Am Chem Soc 2004;126:14773–7.
[10] Hu Z, Jonas AM, Varshney SK, Gohy J-F. J Am Chem Soc 2005;127:6526–7.
[11] Cornelissen JJLM, Fischer M, Sommerdijk NAJM, Nolte RJM. Science 1998;280:1427–30.
[12] Engelkamp H, Middelbeek S, Nolte RJM. Science 1999;284:785–8.
[13] Klok H-A, Jolliffe KA, Schauer CL, Prins LJ, Spatz JP, Moller M, et al. J Am Chem Soc 1999;121:7154–5.
[14] Vauthey S, Santoso S, Gong H, Watson N, Zhang S. Proc Natl Acad Sci USA 2002;99:5355–60.
[15] Santoso S, Hwang W, Hartman H, Zhang S. Nano Lett 2002;2:687–91.
[16] Song Y, Challa SR, Medforth CJ, Qiu Y, Watt RK, Peña D, et al. Chem Commun 2004:1044–5.
[17] Zheng Y, Lin Z, Zakin JL, Talmon Y, Davis HT, Scriven LE. J Phys Chem B 2000;104:5263–71.
[18] Bauer B, Davidson M, Orwar O. Langmuir 2006;22:9329–32.
[19] Gao L, Shi L, Zhang W, An Y, Liu Z, Li G, et al. Macromolecules 2005;38: 4548–50.
[20] Yu K, Eisenberg A. Macromolecules 1998;31:3509–18.
[21] Lu T, Han F, Li Z, Huang J, Fu H. Langmuir 2006;22:2045–9.
[22] Heaven MW, Cave GWV, McKinlay RM, Antesberger J, Dalgarno SJ, Thallapally PK, et al. Angew Chem Int Ed 2006;45:6221–4.
[23] Li L, Liang X, Lin M, Qiu F, Yang Y. J Am Chem Soc 2005;127:17996–7.

[24] Brunsveld L, Folmer BJB, Meijer EW, Sijbesma RP. Chem Rev 2001;101:4071–98.
[25] Kato T. Science 2002;295:2414–8.
[26] Ikkala O, Brinke GT. Science 2002;295:2407–9.
[27] (a) Fenniri H, Deng B-L, Ribbe AE, Hallenga K, Jacob J, Thiyagarajan P. Proc Natl Acad Sci USA 2002;99:6487–92;
(b) Arigon J, Prata CAH, Grinstaff MW, Barthélémy P. Bioconjugate Chem 2005;16:864–72.
[28] Sijbesma RP, Beijer FH, Brunsveld L, Folmer BJB, Irschberg JHKK, Lange RFM, et al. Science 1997;278:1601–4.
[29] Brunsveld L, Vekemans JAJM, Hirschberg JHKK, Sijbesma RP, Meijer EW. Proc Natl Acad Sci USA 2002;99:4977–82.
[30] (a) Fujita N, Yamashita T, Asai M, Shinkai S. Angew Chem Int Ed 2005;44:1257–61;
(b) Duan H, Chen D, Jiang M, Guan W, Li S, Wang M, et al. J Am Chem Soc 2001;123:12097–8.
[31] Liu X, Jiang M, Yang S, Chen M, Chen D, Yang C, et al. Angew Chem Int Ed 2002;41:2950–3.
[32] Hirst AR, Smith DK, Feiters MC, Geurts HPM, Wright AC. J Am Chem Soc 2003;125:9010–1.
[33] Liu Q, Zhang H, Yin S, Wu L, Shao C, Su Z. Polymer 2007;48:3759–70.
[34] Xiao S, Zou Y, Wu J, Zhou Y, Yi T, Li F, et al. J Mater Chem 2007;17:2483–9.
[35] Chen D, Jiang M. Acc Chem Res 2005;38:494–502.
[36] Zhu J, Yu H, Jiang W. Macromolecules 2005;38:7492–501.
[37] (a) Kato T, Fréchet JMJ. Macromolecules 1989;22:3818–9;
(b) Kato T, Fréchet JMJ, Wilson PG, Saito T, Uryu T, Fujishima A, et al. Chem Mater 1993;5:1094–100.
[38] Verma S, Hauck T, EI-Khouly ME, Padmawar PA, Canteenwala T, Pritzker K, et al. Langmuir 2005;21:3267–72.
[39] Fuhrhop J-H, Wang T. Chem Rev 2004;104:2901–38.
[40] Cho B-K, Jain A, Mahajan S, Ow H, Gruner SM, Wiesner U. J Am Chem Soc 2004;126:4070–1.
[41] Yang M, Wang W, Yuan F, Zhang X, Li J, Liang F, et al. J Am Chem Soc 2005;127:15107–11.
[42] Zhou Y, Yan D. J Am Chem Soc 2005;127:10468–9.
[43] Zhou Y, Yan D. Angew Chem Int Ed 2005;44:3223–6.
[44] Menger FM, Angelova MI. Acc Chem Res 1998;31:789–97.
[45] Matsui H, Holtman C. Nano Lett 2002;2:887–9.
[46] Tsafrir I, Caspi Y, Guedeau-Boudeville M-A, Arzi T, Stavans J. Phys Rev Lett 2003;99:38102.
[47] Lee M, Jang D-W, Kang Y-S, Zin Y-C. Adv Mater 1999;11:1018–21.